Atmos. Chem. Phys. Discuss., 11, 13975–14001, 2011
www.atmos-chem-phys-discuss.net/11/13975/2011/
doi:10.5194/acpd-11-13975-2011

Atmospheric Chemistry and Physics Discussions

Solar response in tropical stratospheric ozone: a 3-D chemical transport model study using ERA reanalyses

S. Dhomse[1], M. P. Chipperfield[1], W. Feng[1], and J. D. Haigh[2]

[1]School of Earth and Environment, University of Leeds, Leeds, LS2 9JT, UK
[2]Blackett Laboratory, Imperial College, London, SW7 2AZ, UK

Received: 18 March 2011 – Accepted: 24 April 2011 – Published: 6 May 2011

Correspondence to: S. Dhomse (s.dhomse@see.leeds.ac.uk)

Published by Copernicus Publications on behalf of the European Geosciences Union.

Abstract

We have used an off-line 3-D chemical transport model (CTM), to investigate the 11-year solar cycle response in tropical stratospheric ozone. The model is forced with European Centre for Medium-Range Weather Forecasts (ECMWF) (re)analysis (ERA-40/Operational and ERA-Interim) data for 1978–2005 time period. We have compared the modelled solar response in ozone to observational data from three satellite instruments, Solar Backscatter UltraViolet instrument (SBUV), Stratospheric Aerosol and Gas Experiment (SAGE) and Halogen Occultation Experiment (HALOE). A significant difference is seen between simulated and observed ozone during the 1980s, which is probably due to inhomogeneities in the ERA-40 reanalyses. In general, the model with ERA-Interim dynamics shows better agreement with the observations from 1990 onwards than ERA-40. Overall both standard model simulations are partially able to simulate a "double peak"-structured ozone solar response profile with a minimum around 30 km, and these are in better agreement with HALOE than SBUV or SAGE. The largest model-observation differences occur in the upper stratosphere where SBUV and SAGE show a significant (up to 4 %) solar response whereas the standard model and HALOE do not. This is partly due to a positive solar response in the ECMWF upper stratosphere analysed temperatures which reduces the modelled ozone signal. The large positive upper stratosphere response seen in SAGE/SBUV can be reproduced in a model run with fixed dynamical fields (i.e. no inter-annual meteorological changes). As this run effectively assumes no long-term temperature changes (solar-induced or otherwise) it should provide an upper limit of the ozone solar response. Overall, full quantification of the upper stratosphere ozone solar response is limited by differences in the observed dataset and by uncertainties in the solar response in the stratospheric temperatures. In the lower stratosphere we find that transport by analysed winds, which contain information about the Quasi-Biennial Oscillation (QBO), can lead to a large ozone solar response. However, the run with fixed dynamical fields also produces a positive solar response (up to 2 %) in line with the SAGE and SBUV

observations.

1 Introduction

Quantifying the influence of the solar flux variability on the Earth's climate is very important in order to understand past behaviour and have confidence in predictions of its future evolution (e.g., Steinbrecht et al., 2004; Dhomse et al., 2006). Various mechanisms have been proposed and some are linked with the changes in ozone concentration, based on the observation that largest flux changes occur in the ultraviolet (UV) region (Haigh, 1994). These changes in UV flux can alter ozone production (and destruction) and, as ozone is a radiatively active gas, they can also modify atmospheric dynamics. For a recent review see Gray et al. (2010). However, such a quantification is difficult as stratospheric ozone concentrations are also influenced by various chemical and dynamical processes such as the Quasi-Biennial Oscillation (QBO), meridional circulation, aerosols, greenhouse gases and halogen loading (WMO, 2007). The strong coupling between these processes makes it quite challenging to separate the influence of any individual process. Such a quantification depends on the quality of not only the ozone data, but also the other data sets used to separate the influence of the individual process. Among the most critical is the quality of the meteorological variables used to separate the dynamical influence.

Most of the earlier model studies that quantified the solar response on stratospheric ozone used either two-dimensional (2-D) models (e.g., Brasseur, 1993) or chemistry-climate models (CCMs, e.g., Austin et al., 2008; SPARC, 2010). However, the apparent "double peak" solar response in the stratospheric O_3 profile (Soukharev and Hood, 2006; Remsberg and Lingenfelser, 2010) is still an issue of scientific debate. Nearly all published 2-D models show only one broad peak in solar response in the tropical middle stratosphere (e.g., Haigh, 1994). Although some CCMs are able to reproduce double peak structure of the solar response in the tropical stratospheric ozone the quality of the models' treatment of transport in the lower stratosphere has not been fully investigated. For example, mean age-of-air and tropical upwelling from some these models seems to be inconsistent (Austin et al., 2008; Butchart et al., 2011). Austin et al. (2008) found that a representation of the QBO in CCMs is not necessary in order to generate the lower stratospheric peak although they argued that varying sea surface temperatures (SSTs) were. On the other hand, Schmidt et al. (2010), found they they could produce a lower stratospheric peak in their CCM with fixed SSTs and no QBO.

There are also some additional puzzles about the solar response in the stratosphere. Firstly, using Solar Backscatter UltraViolet instrument (SBUV), Stratospheric Aerosol and Gas Experiment (SAGE) and Halogen Occultation Experiment (HALOE) data, the estimated solar response shown in Fig. 14 from Soukharev and Hood (2006), indicates a minimum solar response in the middle stratosphere with a larger response above and below (see also Fig. 12 in Randel and Wu (2007) and Fig. 3 in Tourpali et al. (2007)). In contrast, using HALOE data for the 1992–2005 time period Remsberg (2008) and Fadnavis and Beig (2010) estimated a maximum solar response near 32–35 km, which decreases in the upper stratosphere. Secondly, most studies which considered temperature show a significant positive solar response in the upper stratospheric temperatures (e.g., Randel et al., 2009; Remsberg, 2009; Frame and Gray, 2010). Direct increases in UV flux can lead to direct increases in both ozone and temperature. Increases in ozone will also increase radiative heating. However, ozone and temperature are anti-correlated in the upper stratosphere and so this feedback (Brasseur and Solomon, 1984) will modify the apparent ozone solar response.

Along with these uncertainties of the representation of the observed solar response, the inability of the models to reproduce the observed solar response in the ozone profile has been linked with the dynamical fields (Kodera and Kuroda, 2002), the aliasing effect of QBO and volcanic eruption (Lee and Smith, 2003) or changes in odd-oxygen due to energetic particles (Callis et al., 2001). However, Hood and Soukharev (2006) pointed out that the effects of odd-nitrogen occur only at higher latitudes. Therefore, the model deficiencies can be linked primarily with the quality of dynamical fields. 2-D models have a simple parameterisations of eddy fluxes while many CCMs are not able

ACPD
11, 13975–14001, 2011

to simulate dynamical features of the tropical stratosphere such as the QBO. In addition many simulations are performed using fixed solar irradiances for solar maximum and solar minimum conditions.

Off-line three-dimensional (3-D) CTMs are computationally inexpensive and can use analysed winds to specify the transport. In some ways these winds are more realistic than a CCM as they are tied to the real state of the atmosphere. On the other hand care is needed when using these winds for long-term studies (for e.g. Feng et al., 2007; Monge-Sanz et al., 2007). Sekiyama et al. (2006) used a 3-D CTM (MJ98-CTM) forced with dynamical fields from a General Circulation Model (GCM), assimilated with ERA-40 winds at every time step, to study the solar response in the stratosphere. They showed that ozone changes are controlled by photochemistry in the upper stratosphere and by dynamics in the tropical lower stratosphere (TLS), with the transition occurring between 10–30 hPa (25–30 km). In this paper we use the SLIMCAT 3-D CTM, forced with European Centre for Medium-Range Weather Forecasts (ECMWF) dynamical fields (ERA-40, ECMWF operational, and ERA-Interim) for a more detailed study to quantify the solar response in tropical ozone. We perform an updated analysis of the ozone profile solar response from two height-resolved satellite data sets: SBUV from McLinden et al. (2009) and SAGE from Randel and Wu (2007). In particular, we investigate the profile of the solar response in tropical ozone in the model and observational data using correlation, composite and regression analysis. Section 2 describes our 3-D model and the experiments performed while Sect. 3 describes the satellite ozone datasets that we have used. The results of the model runs are described in Sect. 4 and our summary is given in Sect. 5.

2 Model experiments

We have used the SLIMCAT 3-D CTM with different meteorological forcings. A detailed description of the model can be found in Chipperfield (1999) and later updates in Chipperfield (2006). SLIMCAT has been extensively validated against various ground-

ACPD
11, 13975–14001, 2011

based and satellite data sets as well used to study short-term and long-term ozone changes (e.g., Chipperfield and Jones, 1999; Sinnhuber et al., 2003; Rex et al., 2004; Chipperfield et al., 2005; Feng et al., 2007; Santee et al., 2008). Some of the key recent improvements relevant for this study are as follows. We have updated the representation of solar flux variability using monthly mean solar solar fluxes from Lean et al. (2001) for all 203 UV-visible spectral bands used in the photochemistry scheme. Reaction rates have been updated from Sander et al. (2006) and we have improved representation of the stratospheric aerosol loading using stratospheric aerosol data from SPARC (2006).

In this study we use a model resolution of $5.6^\circ \times 5.6^\circ$ with $32\sigma - \theta$ levels from the surface to ~60 km and the experiments performed are summarised in Table 1. For run *A_E40*, the model was forced using meteorological fields from ECMWF (re)analyses (ERA-40 (1978–2001) and operational (2002–2005)). During February 2006 the ECMWF operational model underwent significant changes, so we restrict our analysis to the period ending December 2005. It should be noted that the model does not use analysed vertical winds in the stratosphere but rather they are calculated using heating rates for every time step. Run *B_EI* is similar to run *A_E40*, except ERA-Interim dynamical fields are used for the 1989–2005 time period. Run *C_FIX* uses one year of meteorology (fixed from year 2004 using ECMWF operational analysis) repetitively for 27 years.

3 Satellite ozone data

For comparison, we use total ozone from the Total Ozone Mapping Spectrometer (TOMS) and SBUV merged (Revision 5) dataset (Frith et al., 2004) which are monthly zonal mean total ozone values constructed by merging individual TOMS, SBUV/SBUV2 and OMI satellite observations (hereafter "TOMS/SBUV"). We also use SAGE-corrected SBUV ozone profile data from McLinden et al. (2009), which were obtained from ftp://es-ee.tor.ec.gc.ca/pub/SAGE_corrected_SBUV (hereafter "SBUV").

ACPD
11, 13975–14001, 2011

They are constructed by correcting the drifts in individual SBUV instruments and inter-SBUV biases using coincident SAGE I and II observations. We also use SAGE ozone profile data from Randel and Wu (2007), which were obtained from ftp://atmos.sparc.sunysb.edu/pub/sparc/ref_clim/randel/o3data. (hereafter "SAGE"). These are monthly mean ozone data (in DU/km) for altitudes up to 50 km, and are derived from a combination of SAGE I–II satellite data and polar ozonesondes for 1979–2005 time period. For profile comparisons we also use sunrise and sunset measurements from the Halogen Occultation Experiment (HALOE – V19, 1992–2005). Data are included only if the measurement error is less than 100 %. Recently identified corrupted HALOE ozone profiles due to a trip angle problem (C. Brühl, personal communication, 2009), are not used. Monthly mean values are calculated only if there are more than five profiles between 25° S–25° N for a given month. Due to its shorter time span, detailed analysis of HALOE data is not performed here, though we do use it to compare solar maximum and solar minimum conditions.

4 Results and discussion

Figure 1 shows monthly total ozone anomalies from SLIMCAT (runs *A_E40* and *B_EI*) and TOMS/SBUV data averaged between 25° S–25° N. Normalised F10.7 solar fluxes used in our analysis are also shown. Both model runs show reasonable agreement with the satellite data but run *B_EI* agrees better from 1989 onwards, the start of the ERA-Interim data. However, some distinct differences are apparent. First, both model runs show more ozone loss after the Mt. Pinatubo eruption during 1992–1994 although the overestimate is worse in run *A_E40*. Second, a sudden drop in modelled ozone anomalies after 2001 in run *A_E40*, associated with the change in meteorological fields, is also visible. Third, during the 1980s larger differences in modelled ozone anomalies and satellite data are noticeable. It should be noted that recent total ozone retrieval (v8) from both TOMS and SBUV shows good agreement with the ground-based stations (Labow et al., 2004). Hence irregular differences between TOMS/SBUV data

ACPD
11, 13975–14001, 2011

and chemically consistent modelled data highlight the time-varying inconsistencies in dynamical fields used for these runs.

Figure 2 compares tropical (25° S–25° N) monthly ozone anomalies from satellite data (SBUV, HALOE and SAGE) and the SLIMCAT simulations at 4 altitudes. During the mid-1990s modelled ozone anomalies from runs *A_E40* and *B_EI* are generally in good agreement with SBUV, HALOE and SAGE anomalies. As for total ozone, increases in ozone at 25 km from run *A_E40* in the late 1980s overestimate the observations. Sudden changes in profile ozone anomalies after 2001 from run *A_E40* above 40 km are also distinctly visible. A similar drop in ozone anomalies from run *B_EI* are noticeable after 1998 at 50 km. One of the most striking features in Fig. 2 is that at 40 km the modelled ozone anomalies from run *A_E40* show an increasing trend until 1990 and hence they are consistently lower than SBUV data during the early 1980s. This is most probably due to inhomogeneities in ERA-40 data during 1980s (e.g. see Fig. 6 from Dhomse et al., 2008).

Figure 2 also reveals some additional differences in the tropical stratosphere. At 25 km, after the Mt. Pinatubo eruption (1993–1995), both runs *A_E40* and *B_EI* show more ozone loss than the satellite data sets. This may explain the slightly larger modelled ozone solar response in the TLS and is discussed later. As noted earlier, ozone anomalies from run *A_E40* are larger during the 1980s at 25 km. Also, at 30 km HALOE anomalies show more ozone during 1992–1994. Above 40 km, ozone anomalies from run *B_EI* are in better agreement with SBUV, SAGE and HALOE.

Differences in simulated ozone from run *A_E40* and *B_EI* are due to differences in the forcing meteorology used for these two runs. Figure 3a and b shows the differences in simulated tropical ozone and temperature between these two simulations. During 1998–2002 large temperature differences are seen between ERA-40 and ERA-Int at 45–55 km (ERA-40 colder than ERA-Int). In the upper stratosphere ozone has a short photochemical lifetime and is strongly anti-correlated with temperature. Figure 3c and d quantifies this anti-correlation for the modelled ozone and temperature differences between the two runs for 40 km and 55 km, respectively. At 40 km a 1 K increase in

ACPD
11, 13975–14001, 2011
Tropical solar response using a 3-D CTM
S. Dhomse et al.

temperature leads to a 2 % decrease in ozone, while at 55 km a 1 K increase causes a 1 % O_3 decrease. In the lower stratosphere ozone is longer lived and under dynamical control. The largest differences in modelled ozone (up to ±20 %) occur in the tropical lower stratosphere, where differences in temperature are quite negligible. These large differences in ozone must be due to differences in transport (horizontal as well as vertical) in ERA-40 and ERA-Int analysis (also see Chipperfield, 2006; Monge-Sanz et al., 2007).

As noted earlier, stratospheric ozone is strongly influenced by various chemical and dynamical process, and quantifying the solar influence is complicated. Therefore, we have performed correlation, composite and regression analyses to check the robustness of the simulated solar response in the tropical stratosphere. Figure 4 shows the lag correlation between tropical ozone anomalies and the QBO (30 hPa), Southern Oscillation Index (SOI) and F10.7 solar flux. QBO and SOI (Niña 3.4) indices were obtained from CPC data centre (http://www.cpc.noaa.gov/data/indices/). Missing SBUV data above 21 km were interpolated using harmonic analysis. Correlations are shown for 25 months (−12 to +12 months).

Generally the QBO – ozone lag-correlation patterns from SLIMCAT and the satellite data (top panels) are quite similar. As the SAGE data was constructed using a regression model that included QBO terms it shows the largest correlation (up to +0.7) with +6 month lag at 25 km. For SOI (middle panels) the correlation patterns are somewhat different. Ozone anomalies from runs *A_E40* and *B_EI* show a positive correlation (up to 0.3) in the middle stratosphere, while SAGE and SBUV show insignificant correlations throughout the stratosphere. For the F10.7 flux (lower panels) ozone anomalies from both runs *A_E40* and run *B_EI*, show larger positive correlations in the TLS stratosphere with a 3–5 month lag. In the lower stratosphere, SBUV data shows less correlation than SAGE or the model runs. All the datasets show some sort of minimum correlation near 30 km. The largest differences between the datasets occur in the upper stratosphere between 40–50 km. Both SBUV and SAGE data show a large positive correlation whereas the correlation is much less (or even negative) in the model runs

ACPD
11, 13975–14001, 2011

at 50 km.

For the composite analysis, we divide modelled and satellite data into solar maximum and solar minimum months. Months with a normalised F10.7 flux more (less) than 1σ from the mean are categorised as solar maximum (minimum) months. For 1979–2005 (run *A_E40*, SAGE and SBUV) 75 months were categorised as solar maximum and 80 months as solar minimum. For 1989–2005 (run *B_EI*) 44 months each were categorised as solar maximum and minimum. Figure 5 shows the percentage change in ozone for solar maximum minus solar minimum for SBUV, SAGE and HALOE (from Remsberg, 2008). Our analysis of SBUV is similar to SAGE and shows less difference between these datasets than in (Hood et al., 2010). Notably, our analysis shows a positive response around 35 km. This difference in the SBUV analysis with respect to (Hood et al., 2010) could be due to the fact we use data from McLinden et al. (2009), which has been corrected using SAGE, and that we process the data on altitude levels. Both runs *A_E40* and *B_EI* show largest differences in the TLS, where the model shows more ozone during solar maximum than during solar minimum. Minimum ozone differences between solar maximum and solar minimum occur near 30 km, which is in reasonable agreement with most earlier studies (Soukharev and Hood, 2006; Randel and Wu, 2007; Remsberg, 2008). However, above 35 km, differences between the runs *A_E40* and *B_EI* diverge considerably with respect to SAGE and SBUV (and run *C_FIX*) which show up to 4 % ozone difference for solar maximum-minimum months, while runs *A_E40* and *B_EI* (as well as HALOE) show 1–1.5 % ozone difference at these altitudes. Around 50 km, both runs *A_E40* and *B_EI* show negligible ozone difference between solar maximum and solar minimum months, although an increasing difference occurs above this altitude.

Figure 5d shows the solar cycle in ECMWF temperature data calculated by composite analysis for ERA-40 and ERA-Interim. In the mid-upper stratosphere both datasets give a maximum response of about 2.5 K, although the peak in ERA-Interim occurs about 10 km higher altitude than ERA-40. The smaller temperature response in ERA-Interim near 40 km correlates with the larger ozone response here. Similarly, at higher

ACPD
11, 13975–14001, 2011

altitudes the larger temperature response in ERA-Interim is coupled to the smaller ozone response.

Figure 5c also includes results from the 2-D latitude-height model of Brasseur (1993), as presented by (Remsberg, 2008). In the mid-upper stratosphere this model agrees with the results of HALOE and runs *A_E40* and *B_EI*. 2-D models have simplified treatments of dynamics but in this region the main driver for the solar response is photochemistry and temperature. The 2-D model will capture the ozone-temperature feedbacks while our run *C_FIX* quantifies the solar photochemical response against a background atmosphere of fixed temperatures. The negative temperature-ozone correlation in the mid-upper stratosphere will mean that the positive solar temperature response (e.g. through more ozone heating) will reduce the ozone solar response. This negative feedback means that the solar response diagnosed from run *C_FIX* in the upper stratosphere should be an unrealistic upper limit.

Following earlier studies (e.g., WMO, 2007), we also use a multivariate regression model to quantify the solar response in tropical ozone. The statistical model used here is similar to Dhomse et al. (2006), and has the following form:

$$O_3 = \text{constant} + \text{EESC} + \text{QBO}_{30} + \text{QBO}_{50} + \text{aerosols} + \text{solar} + \text{SOI} + \text{residuals}$$

where O_3 are ozone anomalies for the given month at a given altitude. Monthly mean anomalies are calculated by subtracting 27-yr mean values for a given month. Here we use 12 terms for Equivalent Effective Stratospheric Chlorine (EESC) loading, 12 terms for stratospheric aerosol loading and 24 terms for QBO (accounting for both phase and speed of QBO). Eddy heat flux ($\overline{v'T'}$) terms, accounting for the ozone transport to mid-high latitudes (Weber et al., 2003) are not included here, as they may contain some component of solar variability. We use only one term for solar flux variability (F10.7 flux) and one term for SOI. We also apply a Cochrane-Orcutt transformation to the regression equation using an estimate of the auto-correlation with a time lag of one month (Cochrane and Orcutt, 1949). Biases in simulated ozone from run *A_E40* after 2001, are removed by adding a step function in the regression model. For run *C_FIX*,

ACPD
11, 13975–14001, 2011

QBO and SOI terms are removed from the regression model.

Results from the regression model are shown in Figure 6. Overall, the estimated solar response follows the results from the correlation and composite analysis. In the TLS, both runs *A_E40* and *B_EI*, show up to 10 % ozone solar response below 25 km, while SBUV, SAGE and run *C_FIX*, show only up to 4 % response. Recently, Marsh and Garcia (2007) argued that most of the TLS solar response is likely due to ENSO. However, as pointed out by Hood et al. (2010), we also notice that inclusion of ENSO term in our regression model does not show any significant reduction in the magnitude of the solar response in the TLS. So the larger solar response in runs *A_E40* and *B_EI* is most probably due to combinations of more ozone loss (due to aerosols) during solar minimum months and stronger downward mixing of ozone-rich air below 30 km, where the ozone photochemical lifetime increases rapidly from a few months to a few years.

In the middle stratosphere (between 30–45 km) runs *B_EI* and *C_FIX* show much better agreement with SAGE and SBUV data than run *A_E40*. As noted earlier, both profile and total ozone from run *B_EI* is in better agreement with SBUV, SAGE and TOMS/SBUV data. Agreement with the composite analysis in this region adds confidence in the nature of solar response in this region. However, Soukharev and Hood (2006) and Randel and Wu (2007) show negligible (up to 1 %) solar response between 30–38 km, which is similar with run *A_E40*. Noting that both Soukharev and Hood (2006) and Randel and Wu (2007) do not include high stratospheric aerosol loading years and use a different approach to remove QBO interference, the exact cause of differences in estimated solar response from SBUV (Soukharev and Hood, 2006) and SAGE (Randel and Wu, 2007), with this present study is not clear.

Similar to the correlation and composite analyses, in the upper stratosphere (above 45 km) there are significant differences in solar response from the regression model from runs *A_E40* and *B_EI*, and SBUV, SAGE and run *C_FIX*. Runs *A_E40* and *B_EI*, indicate nearly zero solar response near 50 km, which is in agreement with Remsberg and Lingenfelser (2010) (see also Fig. 3c from Fadnavis and Beig, 2010). However, run *C_FIX*, SBUV and SAGE data show up to 4 % solar response in this region, which

ACPD
11, 13975–14001, 2011

is similar to Soukharev and Hood (2006) and Randel and Wu (2007). Remsberg and Lingenfelser (2010) argued that these differences are due to larger negative trends in SAGE data in the upper stratosphere for 1979–2005 period. Randel and Wu (2007) also noted that integrated ozone from SAGE data show larger negative trends than TOMS/SBUV total ozone data.

However, the most striking feature of this analysis is that the solar response from run *C_FIX*, shows much better agreement with SBUV and SAGE data. It shows that solar response in upper stratospheric ozone can be reproduced only if unrealistic (i.e. fixed) dynamical and temperature fields are used. We also note that upper stratospheric ozone is highly sensitive to temperature and chlorine loading. There is significant cooling in the upper stratosphere (increasing greenhouse gases) and reversal in chlorine loading (Montreal Protocol). Changes in chlorine are included in run *C_FIX*, which would lead to a long-term trend even with the fixed meteorology.

5 Summary and conclusions

We have used an off-line 3-D chemical transport model to investigate the solar response in tropical stratospheric ozone. Simulated total ozone from the CTM captures most of long-term and short term ozone variability as observed in TOMS/SBUV data. However, some large differences between satellite and modelled total ozone highlight that there are still some inhomogeneities in ERA-40 reanalyses, especially in the 1980s. Also, total ozone from run *B_EI* (ERA-Interim) shows better agreement with the TOMS/SBUV data than run *A_E40* (ERA-40). Therefore, the estimated solar response in earlier studies based on ERA-40 meteorology might be erroneous.

Similar differences are seen in profile ozone from run *A_E40* during the 1980s. Although ozone anomalies from run *B_EI* show better agreement with SBUV and SAGE data, a sudden drop in ozone above 50 km in ozone from run *B_EI* after 1998 is also noticeable. This is driven by temperature changes which are different between ERA-40 and ERA-Interim. Correlation of model ozone and temperature changes shows that a

Discussion Paper | Discussion Paper | Discussion Paper | Discussion Paper |
ACPD
11, 13975–14001, 2011
Tropical solar response using a 3-D CTM
S. Dhomse et al.
Title Page
Abstract Introduction
Conclusions References
Tables Figures
◀◀ ▶▶
◀ ▶
Back Close
Full Screen / Esc
Printer-friendly Version
Interactive Discussion

1 K temperature decrease leads to a modelled ozone increase of nearly 2 % and 1 % in the middle and upper stratosphere, respectively. In the TLS region, differences in ozone from *A_E40* and *B_EI* are due to differences in transport between ERA-40 and ERA-Interim (Monge-Sanz et al., 2007).

We have investigated the modelled ozone solar response using correlation, composite and regression analyses and compared this with satellite observations. The magnitude and shape of the solar response from SBUV and SAGE are similar, i.e. minimum solar response near 30 km, which increases in the lower and middle stratosphere. The simulated solar response from all the model runs seems to be in reasonable agreement with solar response from SBUV and SAGE in the low-mid stratosphere. Again the response from run *B_EI* agrees somewhat better than run *A_E40* with these datasets in this region. However, our modelled solar response in the middle stratosphere (30–38 km) agrees better with Remsberg (2008) (who used HALOE data) and Remsberg and Lingenfelser (2010) (SAGE 1992–2005) than Soukharev and Hood (2006) (HALOE, SAGE and SBUV) and Randel and Wu (2007) (SAGE). The latter two studies show nearly negligible response between 30–38 km. In contrast, our model shows up to 1–2 % ozone response in this region.

The solar response in TLS ozone from runs *A_E40* and *B_EI* appears to be amplified due to enhanced stratospheric loading during solar minimum months immediately after the eruption of Mt. Pinatubo in 1991. The model then produces a larger signal of low ozone. Also, as ozone and temperature are positively correlated in this region, the positive solar response in TLS temperatures, which implies weaker ascent, will increase the ozone signal (Dhomse et al., 2008; Frame and Gray, 2010). The observed solar response in the TLS ozone from a run with constant meteorological forcing (run *C_FIX*) must be due to downward mixing of ozone-richer air (chemical solar response) to below 30 km, where the ozone photochemical lifetime increases rapidly from a few months to a few years.

For the ozone solar response we see the largest observation-model differences in the upper stratosphere, where both SBUV and SAGE data show a much larger solar response than both runs *A_E40* and *B_EI*. However, we also note that different satellite instruments use different measurement techniques, have retrieval errors and have algorithm limitations (e.g., see Wang et al., 1996; Barthia et al., 2004). There is an apparent positive solar response in both ERA-40 and ERA-Interim temperatures (Frame and Gray, 2010). Randel et al. (2009) and Remsberg (2009) also note positive signals in radiosonde and HALOE temperatures in the tropical upper stratosphere. Hence, the exact nature of the solar response in upper stratospheric ozone from SBUV and SAGE remains unclear. Recently, a negative solar response in upper stratospheric ozone was noted by Haigh et al. (2010).

Finally, we note that model run *C_FIX* with annually repeating meteorology is in excellent agreement with the estimated solar response from SBUV and SAGE data. At lower altitudes this implies that dynamics plays only minor role through downward transport below 30 km to give a secondary solar response in the TLS. As *C_FIX* does not include a QBO, the aliasing effect of solar-QBO-stratospheric aerosol loading does not play any role in modifying the TLS solar response. These results are in disagreement with Lee and Smith (2003) who argued that both QBO and aerosol variations are necessary to obtain the double peak solar response. In the upper stratosphere the photochemically-driven solar response from *C_FIX* is expected to be an upper limit as it ignores the well-known negative feedback between ozone and temperature. The results imply that if true the ozone solar response from SBUV and SAGE must be of photochemical origin but we have not modelled the solar temperature response correctly. The reproduction of observed solar response in upper stratospheric ozone without any dynamical feedback, and the disagreement between satellite datasets, highlights that the quantification of solar response still needs further investigation. Use of newly available ozone data from occultation instruments (such as ACE-FTS) will help us to improve our understanding of the solar response.

Acknowledgements. We thank W. Randel, C. McLinden and E. Remsberg for the SAGE, SBUV and HALOE data. We also acknowledge use of the ECMWF data which was obtained via the BADC. This work was supported by the NERC SOLCLI project and NCEO.

ACPD
11, 13975–14001, 2011

References

Austin, J., Tourpali, K., Rozanov, E., Akiyoshi, H., Bekki, S., Bodeker, G., Bruehl, C., Butchart, N., Chipperfield, M., Deushi, M., Fomichev, V. I., Giorgetta, M. A., Gray, L., Kodera, K., Lott, F., Manzini, E., Marsh, D., Matthes, K., Nagashima, T., Shibata, K., Stolarski, R. S., Struthers, G. H., and Tian, W.: Coupled chemistry climate model simulations of the solar cycle in ozone and temperature, J. Geophys. Res., 113, D11306, doi:10.1029/2007JD009391, 2008. 13977, 13978

Barthia, P., Wellemeyer, C., Taylor, S., Nath, N., and Gopolan, A.: Solar Backscatter (SBUV) Version 8 profile algorithm, in: Proceedings of the Quadrennial Ozone Symposium-2004, edited by: Zerefos, C., 295–296, Athens, Greece, ISBN 960-630-103-6, 2004. 13989

Brasseur, G.: The response of the middle atmosphere to long-term and short-term solar variability: a two-dimensional model, J. Geophys. Res., 98, 23079–23090, 1993. 13977, 14000

Brasseur, G. and Solomon, S.: Aeronomy of the Middle Atmosphere, D. Reidel Publishing Company, 1984. 13978

Butchart, N., Charlton-Perez, A. J., Cionni, I., Hardiman, S. C., Haynes, P. H., Krüger, K., Kushner, P. J., Newman, P. A., Osprey, S. M., Perlwitz, J., Sigmond, M., Wang, L., Akiyoshi, H., Austin, J., Bekki, S., Baumgaertner, A., Braesicke, P., Brühl, C., Chipperfield, M., Dameris, M., Dhomse, S., Eyring, V., Garcia, R., Garny, H., Jöckel, P., Lamarque, J., Marchand, M., Michou, M., Morgenstern, O., Nakamura, T., Pawson, S., Plummer, D., Pyle, J., Rozanov, E., Scinocca, J., Shepherd, T. G., Shibata, K., Smale, D., Teyssédre, H., Tian, W., Waugh, D., and Yamashita, Y.: Multi-model climate and variability of the stratosphere, J. Geophys. Res., 116, D05102, doi:10.1029/2010JD014995, 2011. 13978

Callis, L. B., Natarajan, M., and Lambeth, J. D.: Solar-atmospheric coupling by electrons (SOLACE). 3. Comparisons of simulations and observations, 1979–1997, issues and implications, J. Geophys. Res., 106, 7523–7539, 2001. 13978

Chipperfield, M. P.: Multiannual Simulations with a three-dimensional chemical transport model, J. Geophys. Res., 104, 1781–1805, 1999. 13979

Chipperfield, M. P.: New version of the TOMCAT/SLIMCAT off-line chemical transport model: intercomparison of stratospheric tracer experiments, Q. J. Roy. Meteorol. Soc., 132, 1179–1203, 2006. 13979, 13983

Chipperfield, M. P. and Jones, R. L.: Relative influences of atmospheric chemistry and transport on Arctic ozone trends, Nature, 400, 551–554, 1999. 13980

Chipperfield, M. P., Feng, W., and Rex, M.: Arctic ozone loss and climate sensitivity: updated three-dimensional model study, Geophys. Res. Lett., 31, L11813, doi:10.1029/2005GL022674, 2005. 13980

Cochrane, D. and Orcutt, G. H.: Application of least squares regression to relationships containing autocorrelated error terms, J. Am. Stat. Assoc., 44, 32–61, 1949. 13985

Dhomse, S., Weber, M., Wohltmann, I., Rex, M., and Burrows, J. P.: On the possible causes of recent increases in northern hemispheric total ozone from a statistical analysis of satellite data from 1979 to 2003, Atmos. Chem. Phys., 6, 1165–1180, doi:10.5194/acp-6-1165-2006, 2006. 13977, 13985

Dhomse, S., Weber, M., and Burrows, J.: The relationship between tropospheric wave forcing and tropical lower stratospheric water vapor, Atmos. Chem. Phys., 8, 471–480, doi:10.5194/acp-8-471-2008, 2008. 13982, 13988

Fadnavis, S. and Beig, G.: Solar cycle variability in middle atmospheric ozone over tropics, Int. J. Remote Sens., 31, 565, doi:10.1080/01431160902893535, 2010. 13978, 13986

Feng, W., Chipperfield, M. P., Dorf, M., Pfeilsticker, K., and Ricaud, P.: Mid-latitude ozone changes: studies with a 3-D CTM forced by ERA-40 analyses, Atmos. Chem. Phys., 7, 2357–2369, doi:10.5194/acp-7-2357-2007, 2007. 13979, 13980

Frame, T. H. A. and Gray, L. J.: The 11-yr solar cycle in ERA-40 data: an update to 2008, J. Climate, 23, 2213–2222, doi:10.1175/2009JCLI3150.1, 2010. 13978, 13988, 13989

Frith, S., Stolarski, R., and Barthia, P.: Implications of version 8 TOMS and SBUV data for long-term trend, in: Proceedings of the Quadrennial Ozone Symposium-2004, edited by: Zerefos, C., Athens, Greece, 65–66, 2004. 13980

Gray, L., Beer, J., M., G., Haigh, J., Lockwood, M., Matthes, K., Cubasch, U., Fleitmann, D., Harrison, G., Hood, L., Luterbacher, J., Meehl, G., Shindell, D., van Geel, B., and White, W.: Solar influences on climate, Rev. Geophys., 48, RG4001, doi:10.1029/2009RG000282, 2010. 13977

Haigh, J. D.: The role of stratospheric ozone in modulating the solar radiative forcing of climate, Nature, 370, 544–546, 1994. 13977

Haigh, J. D., Winning, A. R., Toumi, R., and Harder, J. W.: An influence of solar spectral variations on radiative forcing of climate, Nature, 467, 696–699, 2010. 13989

Hood, L. L. and Soukharev, B. E.: Solar induced variations of odd nitrogen: multiple regression analysis of UARS HALOE data, Geophys. Res. Lett., 33, L22805, doi:10.1029/2006GL028122, 2006. 13978

ACPD
11, 13975–14001, 2011

Hood, L. L., Soukharev, B. E., and McCormack, J. P.: Decadal variability of the tropical stratosphere: secondary influence of the El Niño/Southern Oscillation, J. Geophys. Res.,, J. Geophys. Res., 115, D11113, doi:10.1029/2009JD012291, 2010. 13984, 13986
Kodera, K. and Kuroda, Y.: Dynamical response to the solar cycle: winter stratopause and lower stratosphere, J. Geophys. Res., 107, doi:310.1029/2002JD002224, 2002. 13978
Labow, G., McPeters, R., and Barthia, P.: A comparison of TOMS & SBUV version 8 total column ozone data with data from ground, in: Proceedings of the Quadrennial Ozone Symposium-2004, edited by: Zerefos, C., Athens, Greece, ISBN 960-630-103-6, 123–124, 2004. 13981
Lean, J. L., White, O. R., Livingston, W. C., and Picone, J. M.: Variability of a composite chromospheric irradiance index during the 11-year activity and over longer time periods, J. Geophys. Res, 106, 10645–10658, 2001. 13980
Lee, H. and Smith, A. K.: Simulations of the combined effects of solar cycle, quasi-biennial oscillation, and volcanic forcing on the stratospheric ozone changes in recent decades, J. Geophys. Res., 108, 4049, doi:10.1029/2001JD001503, 2003. 13978, 13989
Marsh, D. R. and Garcia, R. R.: Attribution of decadal variability in lower-stratospheric tropical ozone, Geophys. Res. Lett., 34, L21807, doi:10.1029/2007GL030935, 2007. 13986
McLinden, C. A., Tegtmeier, S., and Fioletov, V.: Technical Note: A SAGE-corrected SBUV zonal-mean ozone data set, Atmos. Chem. Phys., 9, 7963–7972, doi:10.5194/acp-9-7963-2009, 2009. 13979, 13980, 13999
Monge-Sanz, B., Chipperfield, M., Simmons, A. J., and Uppala, S. M.: Mean age of air and transport in a CTM: Comparison of different ECMWF analyses, Geophys. Res. Lett., 34, L04 801, doi:10.1029/2006GL028515, 2007. 13979, 13983, 13988
Randel, W. J. and Wu, F.: A stratospheric ozone profile data set for 1979–2005: Variability, trends, and comparisons with column ozone data, J. Geophys. Res., 112, D06303, doi:10.1029/2006JD00733, 2007. 13978, 13979, 13981, 13984, 13986, 13987, 13988, 13999
Randel, W. J., Shine, K. P., Austin, J., Barnett, J., Claud, C., Gillett, N. P., Keckhut, P., Langematz, U., Lin, R., Long, C., Mears, C., Miller, A., Nash, J., Seidel, D. J., Thompson, D. W. J., Wu, F., and Yoden, S.: An update of observed stratospheric temperature trends, J. Geophys. Res., 114, D02107, doi:10.1029/2008JD010421, 2009. 13978, 13989
Remsberg, E. and Lingenfelser, G.: Analysis of SAGE II ozone of the middle and upper stratosphere for its response to a decadal-scale forcing, Atmos. Chem. Phys., 10, 11779–11790,

ACPD
11, 13975–14001, 2011

doi:10.5194/acp-10-11779-2010, 2010. 13977, 13986, 13987, 13988
Remsberg, E. E.: On the response of Halogen Occultation Experiment (HALOE) stratospheric ozone and temperature to the 11-year solar cycle forcing, J. Geophys. Res., 113, D22304, doi:10.1029/2008JD010189, 2008. 13978, 13984, 13985, 13988, 14000
Remsberg, E. E.: Trends and solar cycle effects in temperature versus altitude from the Halogen Occultation Experiment for the mesosphere and upper stratosphere, J. Geophys. Res., 114, D12, 303, doi:10.1029/2009JD011897, 2009. 13978, 13989
Rex, M., Salawitch, R., von der Gathen, P., Harris, N., Chipperfield, M., and Naujokat, B.: Arctic ozone loss and climate change, Geophys. Res. Lett., 31, L04116, doi:10.1029/2003GL018844, 2004. 13980
Sander, S. P., Friedl, R. R., Golden, D. M., Kurylo, M. J., Moortgat, G. K., Keller-Rudek, H., Wine, P. H., Ravishankara, A. R., Kolb, C. E., Molina, M. J., Finlayson-Pitts, B. J., Huie, R. E., and Orkin, V. L.: Chemical Kinetics and Photochemical Data for Use in Atmospheric Studies, JPL Publication 06-2, Jet Propulsion Laboratory, Pasadena, Evaluation Number 15, 2006. 13980
Santee, M. L., MacKenzie, I. A., Manney, G. L., Chipperfield, M. P., Bernath, P., Walker, K. A., Boone, C. D., Froidevaux, L., Livesey, N. J., and Waters, J. W.: A study of stratospheric chlorine partitioning based on new satellite measurements and modeling, J. Geophys. Res, 113, D12307, doi:10.1029/2007JD009057, 2008. 13980
Schmidt, H., Brasseur, G. P., and Giorgetta, M. A.: Solar cycle signal in a general circulation and chemistry model with internally generated quasi-biennial oscillation, J. Geophys. Res., 115, D00I14, doi:10.1029/2009JD012542, 2010. 13978
Sekiyama, T. T., Shibata, K., Deushi, M., Kodera, K., and Lean, J. L.: Recent 22-year simulation using 3-D chemical transport model with reanalysis data, Geophys. Res. Lett., 33, L17812, doi:10.1029/2006GL026711, 2006. 13979
Sinnhuber, B., Weber, M., Amankwah, A., and Burrows, J.: Total ozone during the unusual Antarctic winter of 2002, Geophys. Res. Lett., 30, doi:10.1029/2002GL016798, 2003. 13980
Soukharev, B. E. and Hood, L. L.: Solar cycle variation of stratospheric ozone: multiple regression analysis of long-term satellite data sets and comparisons with models, J. Geophys. Res., 111, D20314, doi:10.1029/2006JD007107, 2006. 13977, 13978, 13984, 13986, 13987, 13988
SPARC: SPARC Assessment of stratospheric aerosol properties (ASAP) SPARC Report No. 4, World Climate Research Programme, WCRP-124,WMO/TD-No.1295, 2006. 13980

ACPD
11, 13975–14001, 2011
Tropical solar response using a 3-D CTM
S. Dhomse et al.

SPARC: SPARC Report on the Evaluation of Chemistry-Climate Models, World Climate Research Programme, WCRP-132,WMO/TD-No.1526, 2010. 13977

Steinbrecht, W., Claude, H., and Winkler, P.: Enhanced upper stratospheric ozone: sign of recovery or solar cycle effect? J. Geophys. Res., 109, 6713–6727, 2004. 13977

Tourpali, K., Zerefos, C. S., Balis, D., and Bais, A. F.: The 11-year solar cycle in stratospheric ozone: comparison between Umkehr and SBUV v8 and effects on surface erythemal irradiance, J. Geophys. Res., 112, D12306, doi:10.1029/2006JD007760, 2007. 13978

Wang, H. J., Cunnold, D. M., and Bao, X.: A critical analysis of Stratospheric Aerosol and Gas Experiment ozone trends, J. Geophys. Res., 101, 12495–12514, 1996. 13989

Weber, M., Dhomse, S., Wittrock, F., Richter, A., Sinnhuber, B., and Burrows, J.: Dynamical control of NH and SH winter/spring total ozone from GOME observations in 1995–2002, Geophys. Res. Lett., 30, 1583, doi:10.1029/2002GL016799, 2003. 13985

WMO: Scientific Assessment of Ozone Depletion: 2006, Global Ozone Research and Monitoring Project Report 50, World Meteorological Organization, Geneva, available online at: http://www.wmo.int/pages/prog/arep/gaw/ozone_2006, 2007. 13977, 13985

Table 1. Solar and dynamical conditions for the model simulations.

Run	Solar fluxes	Dynamics
A_E40	time-varying	ERA-40 + operational
B_EI	time-varying	ERA-Int
C_FIX	time-varying	Perpetual 2004 (operational)

ACPD
11, 13975–14001, 2011

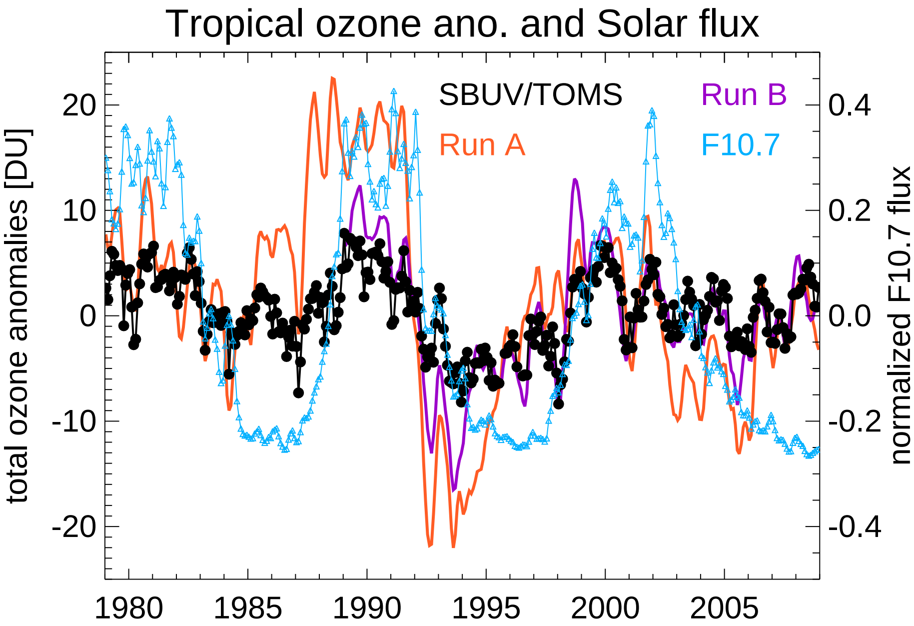

Fig. 1. Comparison of the monthly tropical (25° S–25° N) total ozone anomalies in DU (left hand axis) from the v5 SBUV/TOMS merged ozone dataset (black line) with results from SLIMCAT runs *A_E40* (orange line) and *B_EI* (violet line). The normalised F10.7 solar flux used in the analysis is also shown (light blue line – right hand axis).

ACPD
11, 13975–14001, 2011

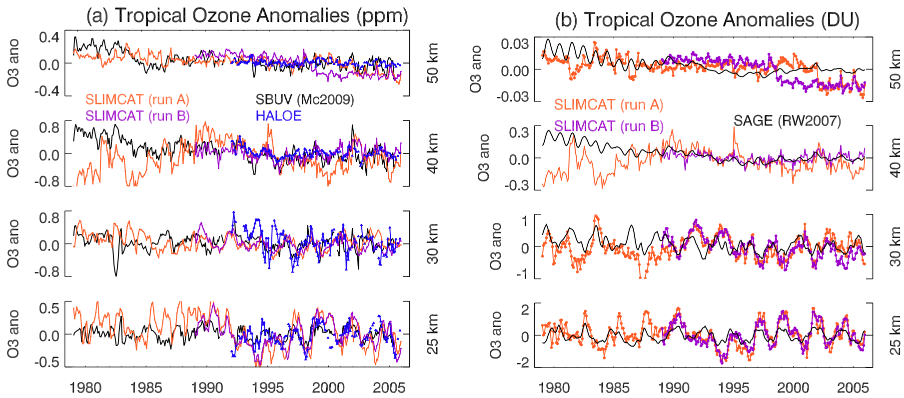

Fig. 2. Comparison of tropical ozone anomalies from SBUV, SAGE II and HALOE with model runs *A_E40* (orange line) and *B_EI* (violet line) for 50 km (top), 40 km (second from top), 30 km (third from top), and 25 km (bottom). Ozone anomalies from HALOE were calculated by combining both sunrise and sunset measurements. Anomalies are shown in ppmv **(a)** and DU/km **(b)**.

ACPD
11, 13975–14001, 2011

Tropical solar response using a 3-D CTM

S. Dhomse et al.

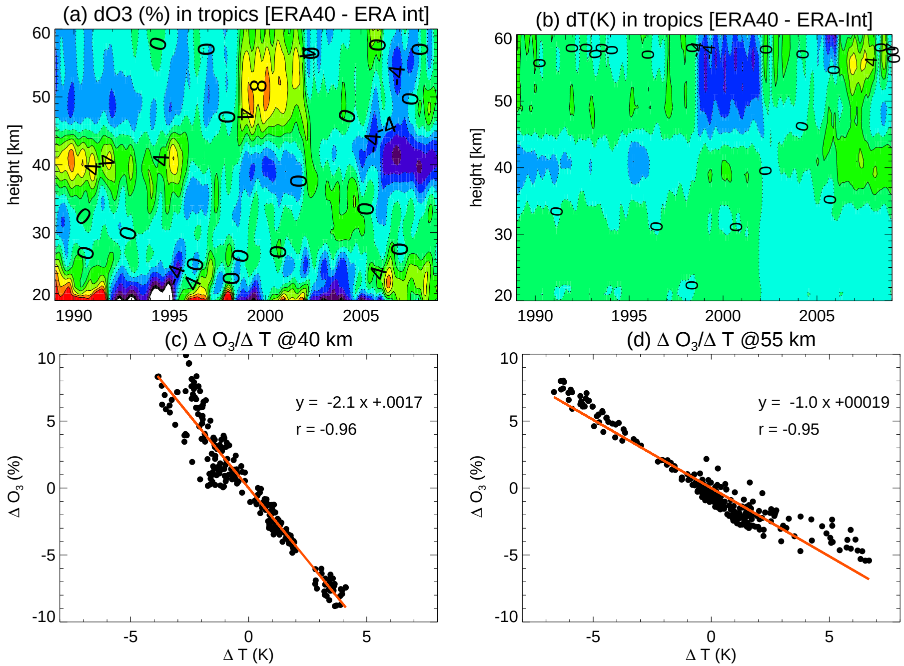

Fig. 3. Tropical differences from run *A_E40* minus run *B_EI* (ERA-40/operational minus ERA-Int) for **(a)** simulated ozone (in %) and **(b)** temperature (K). Contour intervals are 2 % for O_3 and 2 K for temperature. Positive (green to red colours) and negative (blue to violet colours) differences are shown with solid and dashed lines, respectively. Positive contours in Panel **(a)**, indicate more ozone in run *A_E40* whereas one in panel **(b)**, indicate warmer temperatures in ERA-40. Scatter plots of differences in O_3 (%) and differences in T (K) for run *A_E40* minus run *B_EI* at **(c)** 40 km and **(d)** 55 km.

ACPD
11, 13975–14001, 2011

Title Page
Abstract | Introduction
Conclusions | References
Tables | Figures
◂◂ | ▸▸
◂ | ▸
Back | Close
Full Screen / Esc
Printer-friendly Version
Interactive Discussion

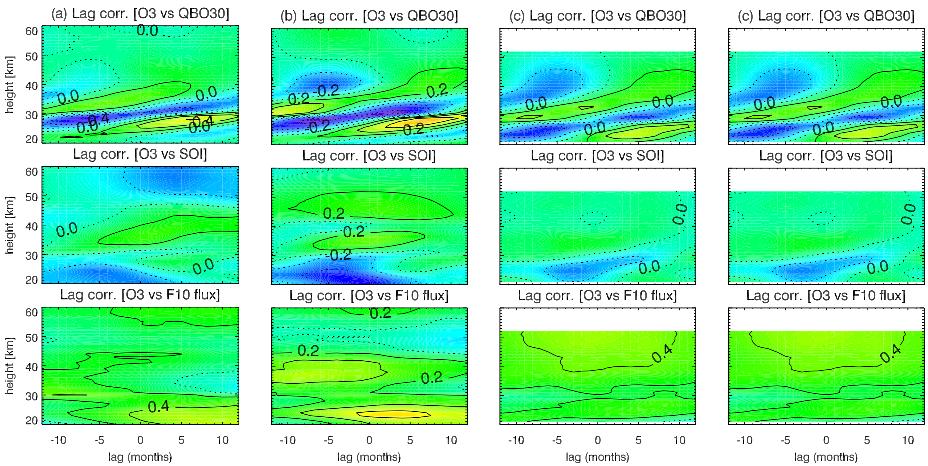

Fig. 4. Lag correlation analysis between tropical ozone anomalies and zonal wind (QBO at 30 hPa), Southern Oscillation Index (SOI) and F10.7 solar flux from −12 to +12 months in top, middle and bottom rows, respectively. Column **(a)** shows the lag-correlation between tropical ozone anomalies from run *A_E40* and 30 hPa QBO, SOI and F10.7 flux for 1979–2005. Column **(b)** shows results from *B_EI* (1989–2005). Column **(c)** shows results from SBUV (1979–2005, from McLinden et al., 2009). Column **(d)** shows results from SAGE (1979–2005, from Randel and Wu, 2007). Positive correlation are shown with solid lines (green and yellow colours), whereas dashed lines indicate negative correlation (blue-violet colours).

ACPD
11, 13975–14001, 2011

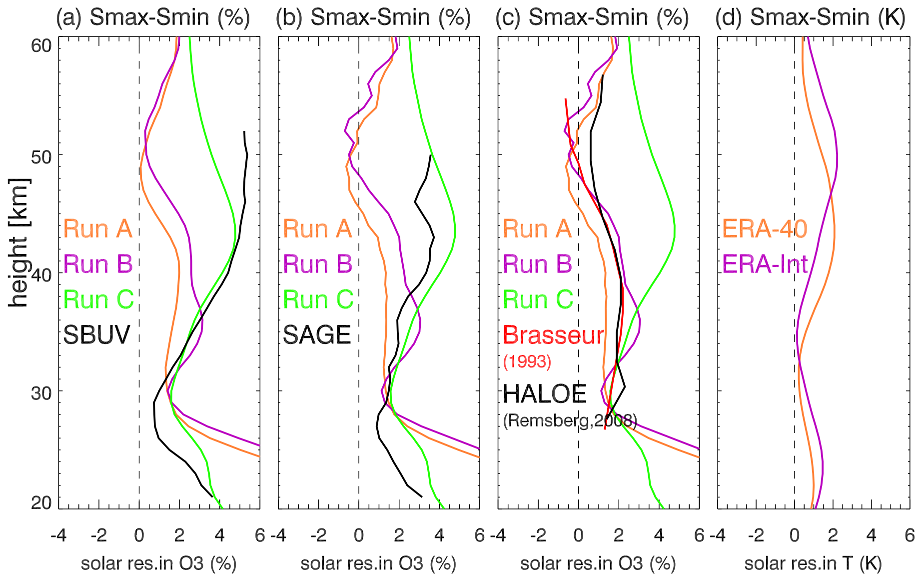

Fig. 5. (a–c) Composite analysis (solar max minus solar min) of the simulated ozone response (in %) from runs *A_E40* (orange line), *B_EI* (violet line) and *C_FIX* (green line). Also shown is the estimated solar response from **(a)** SBUV, **(b)** SAGE, and **(c)** the Brasseur (1993) 2-D model (red) and HALOE data from Remsberg (2008) (black). Panel **(d)** shows the similar composite analysis for temperature (K) from ECMWF ERA-40 and ERA-Interim reanalyses.

ACPD
11, 13975–14001, 2011

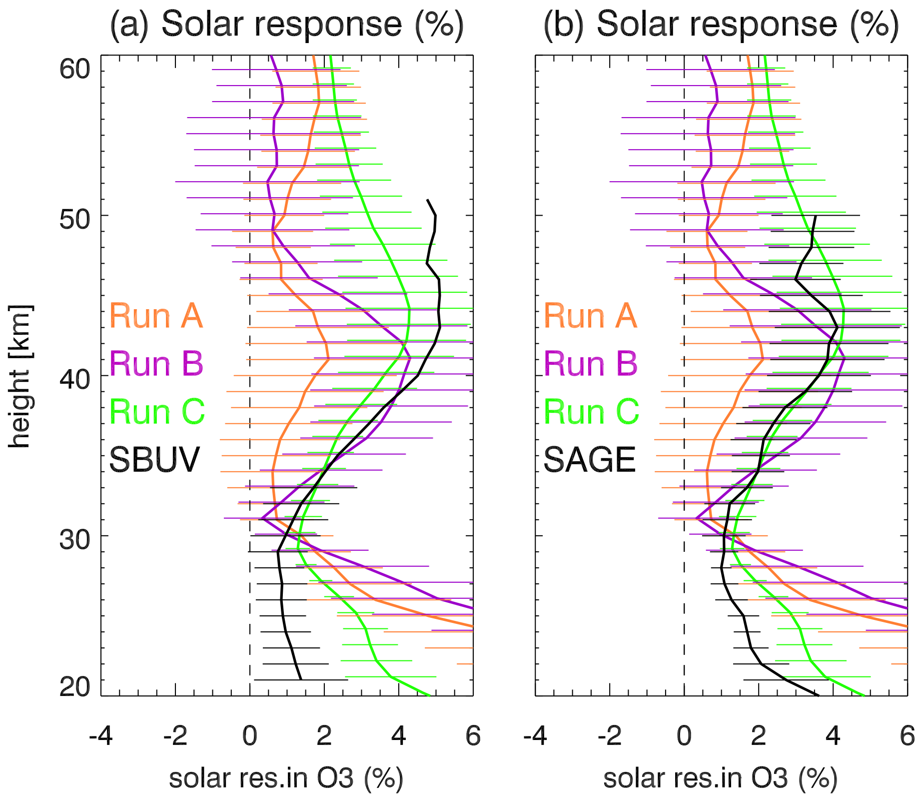

Fig. 6. Solar response in tropical ozone (in %) estimated using regression analysis for model runs *A_E40*, *B_EI* and *C_FIX* compared with observations from **(a)** SBUV and **(b)** SAGE for 1979–2005. The error bars are 2σ.

ACPD
11, 13975–14001, 2011